

Asteroids in the 2 : 1 resonance with Jupiter: dynamics and size distribution

F. Roig,¹*† D. Nesvorný² and S. Ferraz-Mello¹

¹*Instituto Astronômico e Geofísico, Universidade de São Paulo. Av. Miguel Stefano 4200, São Paulo, SP 04301-904, Brazil*

²*Department of Space Studies, Southwest Research Institute, 1050 Walnut St., Suite 426, Boulder, CO 80302, USA*

Accepted 2002 April 26. Received 2002 April 25; in original form 2002 April 4

ABSTRACT

The 2 : 1 mean motion resonance with Jupiter in the main asteroid belt is associated to one of the largest Kirkwood gaps: the so-called Hecuba gap. Centred at about 3.3 au, the Hecuba gap is characterized by a very small number of asteroids when compared to its neighbourhoods. Long-term instabilities caused by resonant planetary perturbations are thought to be responsible for the almost lack of bodies in the gap. However, current observations suggest a significant population of asteroids in the 2 : 1 resonance. The origin of these bodies is puzzling. Do we observe the few lucky survivors of a much larger population formed in the resonance in primordial times? Do the resonant orbits of the observed asteroids have a more recent origin? To understand these issues, we performed numerical simulations of the orbital evolution of both real and fictitious asteroids in the 2 : 1 resonance. Our models include gravitational perturbations by the major planets. Based on the dynamical lifetimes, we classify the observed resonant asteroids into three groups: (i) the Zhongguos, which seems to be stable over the age of the Solar system; (ii) the Griquas, with typical lifetimes in the resonance of the order of some 100 Myr; and (iii) the strongly unstable asteroids, which escape from the resonance in a few 10 Myr or less. Our simulations confirm that the Zhongguos may be primordial asteroids, located in the 2 : 1 resonance since the formation of the Solar system. The dynamics of the Zhongguos constitute a typical example of slow chaotic evolution confined to a small region of the resonance. On the other hand, an analysis of the size distribution of the Zhongguos reveals a rather steep distribution. Such a distribution would not be compatible with a long collisional history, rather suggesting that the Zhongguos are likely to be the outcomes of a recent breakup event. Thus, while dynamics points toward a primordial resonant origin, the size distribution rather points to a recent origin. A possible explanation is that the Zhongguos formed by the cratering/fragmentation of a large resonant or near-resonant asteroid.

Key words: methods: *N*-body simulations – methods: numerical – celestial mechanics – minor planets, asteroids.

1 INTRODUCTION

The distribution of asteroids in the main asteroid belt is characterized by the presence of gaps at certain values of the semi-major axis, which are known as the Kirkwood gaps. The number of asteroids at these gaps is very small relative to other locations in the belt (Kirkwood 1867).

One of the major Kirkwood gaps, the so-called Hecuba gap, delimits the main asteroid belt at the side of larger semi-major axis (~ 3.3 au). The Hecuba gap occurs at the location where the orbital period of an asteroid is half the orbital period of Jupiter.

This configuration is known to dynamicists as the 2 : 1 mean motion resonance with Jupiter. The gap most likely originated as a consequence of the global stochasticity of the resonance (Ferraz-Mello 1994; Michtchenko & Ferraz-Mello 1995, 1996; Nesvorný & Ferraz-Mello 1997a; Moons, Morbidelli & Migliorini 1998), being gradually depleted over the age of the Solar system.

Nevertheless, a small population of resonant asteroids is observed in the gap at present (Morbidelli 1996; Nesvorný & Ferraz-Mello 1997b; Roig & Ferraz-Mello 1999a). Populations of resonant minor bodies are thought to have a cosmogonic origin. The Trojans in the 1 : 1 mean motion resonance with Jupiter were most probably captured during the accretion of Jupiter mass (Marzari & Scholl 1998a,b). The Plutinos in the 2 : 3 mean motion resonance with Neptune are likely to have been captured by the shift of resonances induced by the planetary migration during the late stages

*E-mail: froig@on.br

†Present address: Observatório Nacional, Rua Gen. José Cristino 77, Rio de Janeiro, RJ 20921-400, Brazil.

of the formation of Uranus and Neptune (Malhotra 1995, 1996). The Hildas in the 3 : 2 resonance with Jupiter also constitute a primordial population (Nesvorný & Ferraz-Mello 1997b). There are several large asteroids ($D > 100$ km) among its members whose collisional lifetimes would be much larger than the age of the Solar system (Farinella & Davis 1992). Moreover, all the Hildas seem to have the same chemical composition (they are classified as D-type asteroids), which points to a common process of formation inside the 3 : 2 resonance.

On the other hand, the asteroids in the 2 : 1 resonance have typical sizes smaller than 20 km, which implies collisional lifetimes ~ 1 Gyr. Thus, these bodies are unlikely to be primordial objects in the resonance (Morbidelli 1996; Moons et al. 1998). However, simulations of their evolution seem to indicate that they could survive in resonant orbits at least over 1 Gyr (Morbidelli 1996). Such apparent long-term stability indicates that a primordial origin cannot be ruled out and is worth of further analysis. Unfortunately, the taxonomic classification of these asteroids is unknown, and by now the discussion on their origin can only rely on long-term simulations of the resonant dynamics.

The Hecuba gap is centred at 3.27 au, and is about 0.2 au wide. The number of asteroids observed in the gap is very small when compared with its immediate neighbourhoods. At smaller semi-major axes ($3.1 < a < 3.2$ au), a large number of asteroids is observed, most of them being members of the Themis family (Zappalà et al. 1995). At larger semi-major axes ($3.35 < a < 3.45$ au), the number of objects rises due to the presence of the so-called Cybele's group.

For many years, it was believed that the Hecuba gap was totally depleted of asteroids. By the middle of the 20th century, only one asteroid, (1362) Griqua, was known to reside in the 2 : 1 resonance.¹ The known population began to grow from the 1970s onwards, when the asteroids (1921) Pala and (1922) Zulu were discovered. During the next 20 yr, the number increased, and by the beginning of the 1990s it reached the modest value of some 10 objects. This figure contrasted with the large number of asteroids of the Hilda group, in the 3 : 2 resonance with Jupiter, which by the same epoch accounts for more than 80 objects (Nesvorný & Ferraz-Mello 1997b; Ferraz-Mello et al. 1998b).

This remarkable observational difference between the main first order resonances in the asteroid belt (2 : 1 and 3 : 2), has been explained by the slow chaotic phenomena acting in these resonances. On one hand, the chaos in the 3 : 2 resonance is weak enough to allow a large population of asteroids to survive over the age of the Solar system. On the other hand, the chaos in the 2 : 1 resonance is strong enough to significantly deplete the primordial resonant population (Michtchenko & Ferraz-Mello 1997; Nesvorný & Ferraz-Mello 1997a,b; Ferraz-Mello, Michtchenko & Roig 1998a; Ferraz-Mello et al. 1998b). Nevertheless, several new asteroids were discovered in the 2 : 1 resonance as a consequence of modern observational surveys during the last decade. The 10 objects known in 1990 became 25 in 1996 and more than 50 in 2001 (objects with well known orbits).

The existence of such population of asteroids in the 2 : 1 resonance raises the question of *whether these objects are the remnants of a large primordial resonant population* (like the Hildas or the Plutinos), or *whether their resonant orbits have a more recent origin*.

Another question refers to the possible link of these resonant asteroids to other populations of minor bodies. It has been pro-

posed that the asteroids could have been injected in the resonance by the fragmentation of asteroid (24) Themis at ~ 3.15 au (Morbidelli et al. 1995). Thus, they would be the resonant counterpart of Themis family. However, it is not clear whether such an event can provide the necessary ejection velocities to put the asteroids in their present resonant orbits (Benz & Asphaug 1999). On the other hand, the 2 : 1 resonance is a source of planet crossing asteroids, mainly Jupiter crossing bodies (Moons et al. 1998; Roig & Ferraz-Mello 1999a). This opens a possible link between the resonant asteroids in the Hecuba gap and the Jupiter family comets, which is worth of attention.

The purpose of this paper is to study the current dynamics of the asteroidal population in the 2 : 1 resonance, and their size distribution. Our aim is to better understand the internal dynamics of the resonance and the chaotic phenomena that rules the long-term evolution of these asteroids. We also intend to provide some clues about the possible origin of the resonant asteroids.

The paper is organized as follows. In Section 2 we describe the population of presently observed resonant asteroids, and analyse their orbital distribution and short-term stability. In Section 3 we study the long-term dynamics inside the 2 : 1 resonance. We use N -body integrations and Monte Carlo simulations to trace the evolution of a hypothetical primordial population of asteroids. We briefly discuss the role of non-planetary perturbations, such as the Yarkovsky effect (Farinella & Vokrouhlický 1999) and gravitational scattering by main belt asteroids. In Section 4, we analyse the size distribution of the resonant asteroids. Finally, Section 5 contains our conclusions.

2 THE RESONANT POPULATION

The dynamics of the 2 : 1 resonance is characterized by the libration around 0 of the resonant angle:

$$\sigma = 2\lambda_J - \lambda - \varpi, \quad (1)$$

where λ and ϖ are the mean longitude and the longitude of perihelion, respectively, and the subscript J refers to Jupiter. The libration of σ is coupled with the oscillation of the semi-major axis around the resonant value, $a_{\text{res}} \simeq 3.27$ au. We used this property to identify the resonant asteroids. We considered all the numbered and unnumbered multi-oppositional asteroids listed in the asteroid data base of Lowell Observatory by 2001 October (<ftp://ftp.lowell.edu/pub/elgb>), the semi-major axis and eccentricity of which fell within the limits indicated by dot-dashed lines² in Fig. 1. We numerically integrate these asteroids over 10 000 yr, and plot the evolution of their a and σ . We identified 53 asteroids with confident orbits (Holvorcem, personal communication), for which the resonant angle librates around 0 and the semi-major axis oscillates around 3.27 au. Their orbital elements are shown by triangles in Fig. 1. We further analysed these resonant asteroids to determine their orbital distribution (Section 2.1) and lifetimes (Section 2.2) in the resonance.

2.1 Orbital distribution

Fig. 1 shows the instantaneous values of the orbital elements at a given Julian date. These osculating elements are largely affected by periodic oscillations due to planetary perturbations, and are useless to access the orbital distribution of the resonant asteroids. Actually,

²These limits were chosen empirically by a trial and error approach, and are such that the orbital elements of any resonant asteroid are located within them.

¹In 1928, the first asteroid was discovered in the resonance, but then it was lost. The body was re-discovered in the 1980s and named (3789) Zhongguo.

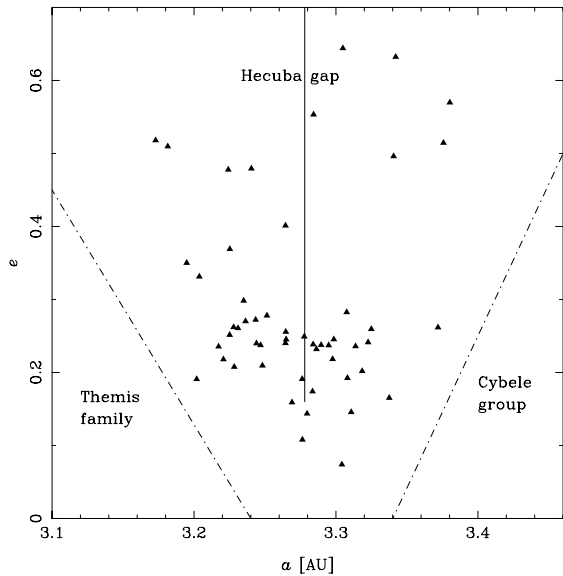


Figure 1. The orbital elements of resonant asteroids in the Hecuba gap. The full vertical line marks the approximate location of the 2 : 1 Jovian resonance. The dashed-dotted lines are the boundaries of our search criteria to identify the resonant bodies.

the location of the asteroids in the resonance is well represented by the so-called *proper elements* (Milani & Knežević 1994; Knežević & Milani 2000). Proper elements are useful to determine if the asteroids are clustered in some special way. Such clusters are usually identified as asteroidal families (Zappalà et al. 1990, 1995). Their members are believed to have a common origin.

Proper elements are constants of motion of a dynamical system. They only exist if the system is integrable. For non-integrable systems, proper elements can still be defined (e.g. Milani & Knežević 1990), but they are no longer constants. If the system is weakly chaotic (nearly integrable), the proper elements vary very little over long intervals of time, oscillating around a mean constant value. However, if the motion is highly chaotic, the proper elements can show large variations, and their mean values can drift in time. The time variation of the proper elements is sometimes referred to as chaotic diffusion, and is useful to quantify the chaoticity (or non-integrability) of an orbit.

In practice, the proper elements can be substituted by certain quantities which have similar properties, i.e. they are almost constant with time for regular orbits, and they show larger variations for chaotic orbits. In the non-resonant case, these quantities are the running averages of the time-series of the orbital elements, a , e , and I , over very long time-spans (e.g. Morbidelli & Nesvorný 1999). In the resonant case, we use the average amplitude of libration instead of the average semi-major axis (e.g. Schubart 1982; Bien & Schubart 1987), as the latter is the same for all the resonant orbits ($\equiv a_{\text{res}}$). These averaged elements can be used instead of the proper elements to detect chaotic diffusion. From here in after, we will refer to the averaged orbital elements as the *pseudo-proper elements*.

Alternatively to the use of running averages, pseudo-proper elements can be defined by the successive intersections of the orbit with a representative surface. This surface must be such that a regular orbit always intersects it at about the same place. Conversely, the intersections of a chaotic orbit have to scatter on the surface. Thus, the pseudo-proper elements can be obtained from the average value of the successive intersections. Moreover, the dispersion of these intersections provides a rough estimate of the chaotic diffusion.

In the case of the 2 : 1 resonance, a representative surface is defined by the following conditions:

$$\sigma = 0, \quad \varpi - \varpi_J = 0, \quad \Omega - \Omega_J = 0, \quad (2)$$

where Ω is the longitude of node (e.g. Michtchenko & Ferraz-Mello 1996). In practice, these conditions are difficult to satisfy simultaneously. Thus, we use the less restrictive conditions

$$\sigma \simeq 0, \quad \varpi - \varpi_J \simeq 0, \quad (3)$$

leaving $\Omega - \Omega_J$ unspecified. For most resonant asteroids, equations (3) are satisfied with a precision of $\pm 5^\circ$ in both angles.

To compute the intersections in this representative surface, we integrated the orbits of the 53 resonant asteroids over 0.2 Myr. We used the symplectic integrator SWIFT (Levison & Duncan 1994). We took into account perturbations by four major planets. The time-series of osculating elements were passed through a digital filter to remove the short-period variations related to Jupiter's orbital motion. The resulting filtered elements a , e , I , were registered each time $|\sigma| \leq 5^\circ$ and $|\varpi - \varpi_J| \leq 5^\circ$. These values were further grouped in two sets: (i) a set with $a < a_{\text{res}}$, corresponding to $\dot{\sigma} < 0$, and (ii) a set with $a > a_{\text{res}}$, corresponding to $\dot{\sigma} > 0$. Whenever $\varpi - \varpi_J \simeq 0$, the first set corresponds to the minima of a and the maxima of e , while the second one corresponds to the maxima of a and the minima of e . Moreover, for weakly chaotic orbits at intermediate eccentricities ($0.2 < e < 0.3$), the condition $\Omega - \Omega_J \simeq 0$ normally corresponds to the maxima of I . Then, among the various intersections of the orbit with the representative surface, we chose the one with $a = a_{\text{min}}$, $e = e_{\text{max}}$ and $I \sim I_{\text{max}}$. This intersection defined our pseudo-proper elements, a_p , e_p , I_p . The other intersections (corresponding to smaller I) were used to estimate the rms of the pseudo-proper elements.

The pseudo-proper elements of the resonant asteroids are shown in Fig. 2. We indicate the names of several low-numbered asteroids. Grey and black dots identify the stable and unstable objects, respectively. The stability criteria and the lifetimes of the asteroids are detailed in Section 2.2. Fig. 2(a) also shows the location of the resonance centres a_{res} (full vertical line at about 3.27 au), and the left border of the resonance (bold line). The amplitude of libration, A_σ , is roughly proportional to $|a_p - a_{\text{res}}|$. We have also plotted the approximate location of the ν_{16} secular resonance, where the nodal precessional rate of the asteroid is equal to the nodal precessional rate of Jupiter (dashed line labelled ν_{16}). The regions above and to the left of the instability border (dotted-dashed line labelled IB) are dominated by the strong chaos generated by the overlap of the ν_5 and ν_6 secular resonances and Kozai resonance (Morbidelli & Moons 1993; Nesvorný & Ferraz-Mello 1997a).

The error bars in Fig. 2 represent the standard deviations σ_a , σ_e , σ_I of the pseudo-proper elements. For most asteroids, the error bars are satisfactory. Exceptions are the chaotic asteroids (black dots near the IB line), which showed significant variations of the pseudo-proper elements over the integration time-span (0.2 Myr). We do not show the error bars of the strongly chaotic asteroids which intersected the representative surface only once. Fig. 2 is a portrait of the present orbital distribution of the resonant asteroids.

In Fig. 2, we can see that nearly all asteroids are located at the left side of the ν_{16} resonance. The central region, between the ν_{16} line and the resonance centre, is not populated. This is likely to be a consequence of the presence of chaotic three-body mean motion resonances involving Jupiter and Saturn (Ferraz-Mello et al. 1998a). The stable asteroids (grey dots) are located at $0.2 < e_p < 0.3$ and $I_p < 5^\circ$. Their small standard deviations are compatible with a quite regular behaviour (Morbidelli 1996). The lowest-numbered stable

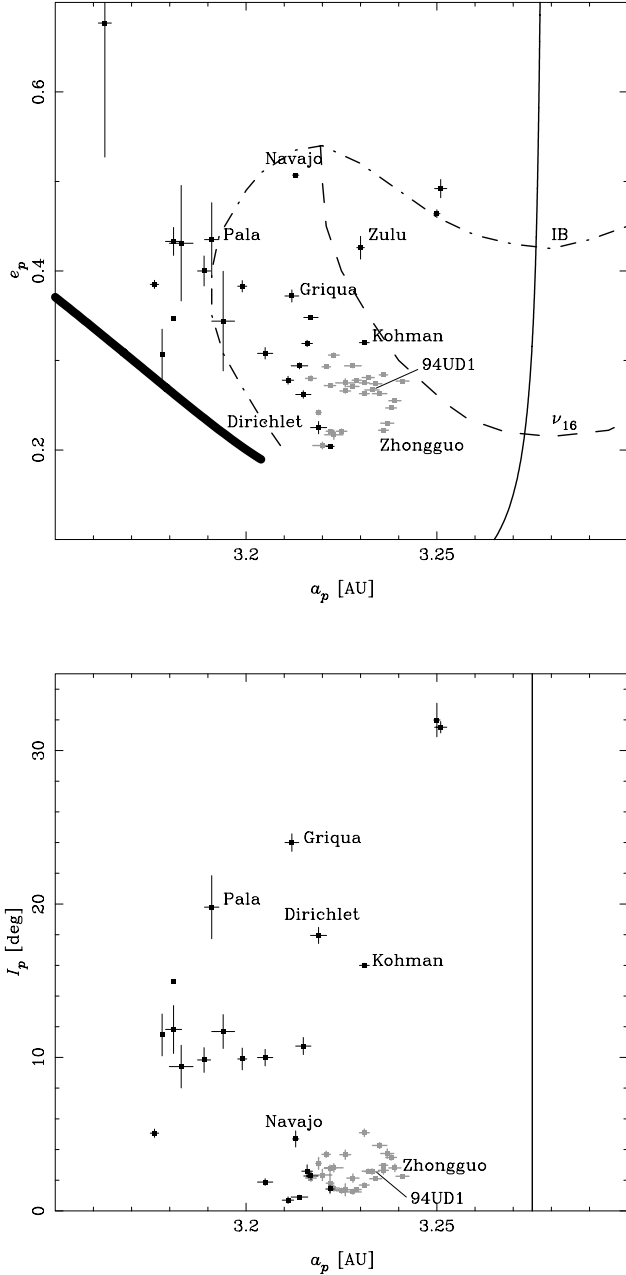


Figure 2. Pseudo-proper elements of resonant asteroids in the Hecuba gap. Grey and black dots distinguish asteroids according to their lifetimes (Section 2.2, Fig. 4). The error bars are the standard deviations of the pseudo-proper elements. Both panels show the location of the resonance centres (full vertical line). The top panel also shows the location of the left resonant border (bold line), ν_{16} secular resonance, and instability border (IB).

asteroid is (3789) Zhongguo, and this is why these bodies are usually referred to as ‘the Zhongguos’ or the ‘Zhongguo group’. Among the Zhongguos, we may clearly identify two clusters, as follows.

(i) The first one is centred at about $a_p \simeq 3.23$ au, $e_p \simeq 0.28$ and $I_p \simeq 2^\circ$, and has ~ 15 members. The lowest-numbered member of this cluster is (11097) 1994 UD1. It is worth noting that (3789) Zhongguo is not a member of this cluster.

(ii) The second cluster is observed at $a_p \simeq 3.22$ au, $e_p \simeq 0.22$ and $I_p \simeq 2^\circ$, and has ~ 5 members. The main member of this cluster is an unnumbered asteroid: 1975 SX. This small cluster overlaps with

the position in a_p, e_p of asteroid (11665) Dirichlet (black dot), but this latter object has a much higher I_p .

To verify that these clusters are not an artefact of our pseudo-proper elements’ computations, we tested the robustness of our method. We re-calculated the pseudo-proper elements using a different approach, and compared the results with Fig. 2. As the angular conditions of the representative surface are related to minima of a and maxima of e, I , the new approach consists of the computation of the running maxima and minima over the time-series of filtered elements (e.g. Morbidelli 1996, 1997). Fig. 3 compares the pseudo-proper elements determined from equation (2) over 0.2 Myr (in the abscissas) with those determined as the extrema of the orbital elements over 10 Myr (in the ordinates). The dashed lines are the identity function. We can see a very good agreement between both sets of pseudo-proper elements. Only for a few chaotic asteroids, we observe large discrepancies due to the different time-spans used in each method.

2.2 Lifetimes

We quantified the stability of the 53 resonant asteroids by direct numerical simulation of their evolution over 520 Myr. We used the symplectic integrator SWIFT, and took into account perturbations by four major planets. The asteroids were discarded from the simulation when: (i) reached a perihelic distance < 0.01 au, (ii) reached a value of $a > 20$ au, or (iii) had an encounter within 0.01 Hill’s sphere to a planet. The lifetime of an asteroid was defined as the time it remained elapsed before its removal. In most cases, the discarded asteroids had escaped from the 2 : 1 resonance a few Myr before their nominal lifetime.

Fig. 4 shows the lifetimes of the resonant asteroids in dependence of a_p . We can see that asteroids near the resonant border ($a_p < 3.21$ au) have the shortest lifetimes. In many cases, these bodies escape from the resonance in less than 20 Myr. Table 1 lists the asteroids with lifetimes shorter than 100 Myr. We call these short-lived asteroids the ‘strongly unstable’ population.

Asteroids with lifetimes between 100 and 500 Myr are listed in Table 2. The list includes (1362) Griqua, (3688) Navajo and (11665) Dirichlet. Most of them are located within $3.21 < a_p < 3.22$ au. Some of them have proper inclinations larger than 10° , like (4177) Kohman, which moves in the ν_{16} resonance. We call these asteroids the ‘marginally unstable’ population, or simply ‘the Griquas’. Finally, 26 asteroids survived the simulation time-span (520 Myr), and are listed in Table 3. These asteroids are the ‘stable’ population or ‘Zhongguos’.

The transition between the stable and marginally unstable populations is not clear because the limit of 520 Myr is quite arbitrary. It is difficult to say how many asteroids would be discarded if we push the simulation up to 1 Gyr or more. Actually, the simulations by Morbidelli (1996) showed that (3789) Zhongguo does not survive in the 2 : 1 resonance for more than 1 Gyr. In any case, this classification of the resonant population in Zhongguos, Griquas and strongly unstable asteroids will prove useful to better interpret the results of the next sections.

3 LONG-TERM STABILITY

In this section we analyse and discuss the long-term stability of the Zhongguos, aiming to determine whether these asteroids have lifetimes shorter than the age of the Solar system, or whether they can survive inside the 2 : 1 resonance over 4.5 Gyr. This subject is

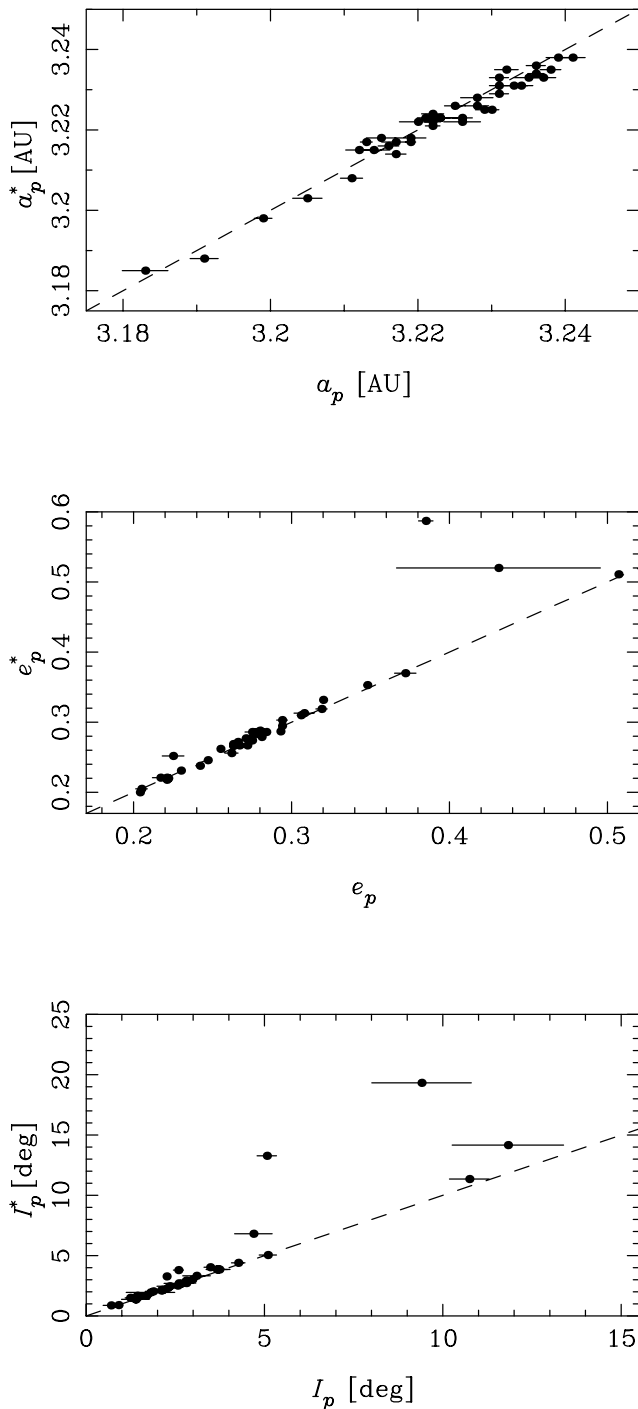


Figure 3. Comparison between pseudo-proper elements a_p , e_p , I_p determined using the representative surface method, and pseudo-proper elements a_p^* , e_p^* , I_p^* computed as the minimum of a and the maxima of e and I over 10 Myr. The agreement between both independent methods is remarkable.

important to determine if the Zhongguos may be primordial objects in the resonance.

Our approach is based on the long-term numerical integration of fictitious resonant orbits. We analysed fictitious instead of real asteroids because this allows to sample the dynamics of an extensive region of the resonance, not only restricted to the small region occupied by the Zhongguos. The 100 fictitious test particles were distributed in a grid of initial conditions in the range $3.205 \leq a \leq$

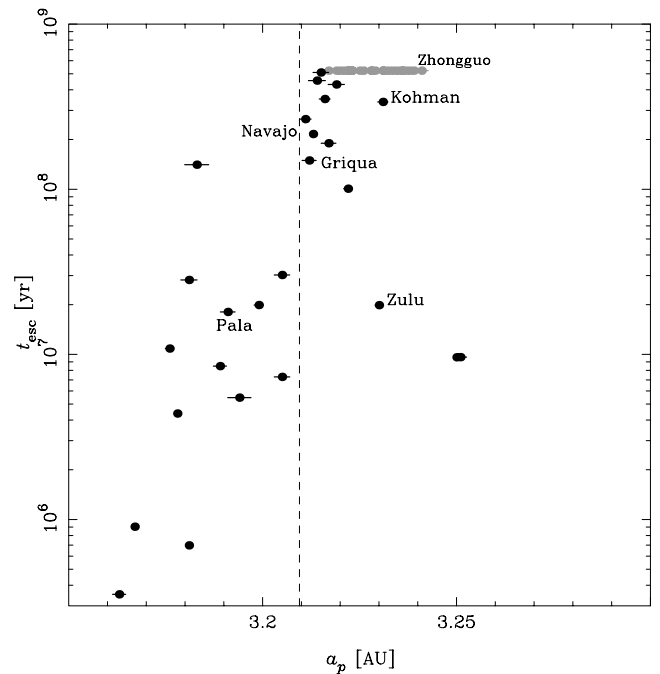


Figure 4. Lifetimes of resonant asteroids in the Hecuba gap. Grey dots denote objects that survived over 520 Myr. For escaping asteroids (black dots), the actual lifetimes inside the 2 : 1 resonance can be smaller than the values shown here. The dashed line at $a_p \simeq 3.21$ au marks the approximate transition limit from marginal to strong instability. See text for details.

3.286 au; $\Delta a = 0.009$ au, and $0.22 \leq e \leq 0.40$; $\Delta e = 0.02$. The initial inclinations were set equal to 0, and the remaining initial angles were chosen such that $\sigma = 0$; $\varpi - \varpi_j = 0$ and $\Omega - \Omega_j = 0$ for all particles. The simulation spanned 4 Gyr and took into account perturbation of four major planets. We used the symplectic integrator SWIFT, with a time-step of 0.08 yr. Particles were discarded following the criteria described in Section 2.2.

Fig. 5 shows the initial orbits of the simulation, shaded according to their survival time. Dark colour denotes short-lived orbits; blank rectangles correspond to test orbits that survived 4 Gyr. We also plot in this figure the resonance centre and border, the IB line and ν_{16} resonance, as well as four dotted lines, denoted N_1, \dots, N_4 , which correspond to different values of

$$N = \sqrt{a}(-2 + \sqrt{1 - e^2} \cos I). \quad (4)$$

This quantity is an integral of motion of the averaged circular restricted three-body problem. The actual motion of resonant asteroids roughly follows these lines, being symmetrical with respect to the resonance centre (Ferraz-Mello 1994). In Section 3.1, this property will be exploited to construct a random-walk model of the resonant dynamics.

Fig. 5 provides clear evidence that some orbits survive inside the resonance over the age of the Solar system. This result is a major achievement compared with previous works on the subject (Morbidelli 1996; Nesvorný & Ferraz-Mello 1997a,b; Moons et al. 1998), that only provided partial or weak evidence of this long-term stability. In our simulations, about 36 per cent of the initial orbits at $3.21 < a < 3.25$ au and $0.20 < e < 0.33$ survived over 4 Gyr. This is precisely the same region occupied by the pseudo-proper elements of the Zhongguos. However, about 25 per cent of the initial orbits at $3.25 < a < 3.29$ au and $0.20 < e < 0.34$ also survived after 4 Gyr, but no asteroid is observed with pseudo-proper elements in that

Table 1. The strongly unstable asteroids observed in the 2 : 1 resonance by October 2001. Columns 1 and 2 identify the object. Columns 3 to 5 show the pseudo-proper elements calculated from equation (3) with $\dot{\sigma} > 0$. Columns 6 to 8 show the standard deviations of the pseudo-proper elements. These are left blank for some asteroids with highly chaotic orbits. Column 9 show the lifetimes. Column 10 indicates other characteristics of the resonant motion: ν_5 denotes the secular resonance between the perihelia of the asteroid and Jupiter, ‘K’ stands for the Kozai resonance, ‘A’ means that the asteroid alternatively moves inside and outside the 2 : 1 resonance. Column 11 gives the estimated diameter, assuming an albedo $A = 0.05$.

No.	Name	a_p [au]	e_p	I_p [°]	σ_a [au]	σ_e	σ_I [°]	t_{life} [$\times 10^4$ yr]	Other	D [km]
1921	Pala	3.191	0.435	19.793	0.0019	0.0413	2.0576	1807.5		8.3
1922	Zulu	3.230	0.426	37.900	0.0010	0.0127	0.3078	1985.9		21.9
5201	Ferraz-Mello	3.100	0.531	4.984	–	–	–	1.8	A	6.6
5370	Taranis	3.205	0.703	9.989	0.0020	0.0015	0.5432	730.4	ν_5	4.4
8373	Stephengould	3.251	0.492	31.518	0.0016	0.0102	0.3687	962.3		10.5
9767	Midsomer Norton	3.167	0.784	64.981	0.0006	0.0588	3.7424	90.4	K, A	3.2
23577	1995 DY8	3.205	0.308	1.880	0.0020	0.0064	0.2239	3025.7		8.7
26166	1995 QN3	3.250	0.464	31.992	0.0008	0.0044	1.0954	959.5		2.4
	1977 OX	3.181	0.347	14.943	–	–	–	69.8	ν_5	5.5
	1994 JC	3.163	0.677	67.844	0.0017	0.1497	19.4343	35.2	K, A	5.8
	1998 KY30	3.194	0.344	11.687	0.0030	0.0557	1.1027	547.5	ν_5 , A	12.0
	1999 XY223	3.176	0.385	5.064	0.0011	0.0046	0.2726	1084.0	ν_5	7.2
	2000 EU170	3.199	0.383	9.903	0.0012	0.0063	0.7103	1989.0		11.5
	2000 JV60	3.181	0.433	11.824	0.0021	0.0157	1.5629	2822.3	ν_5	2.2
	2000 WZ161	3.178	0.307	11.463	–	0.0280	1.3630	438.0		12.0
	9593 P-L	3.189	0.400	9.836	0.0017	0.0167	0.8051	848.2	K	13.2

Table 2. The marginally unstable asteroids (Griquas) observed in the 2 : 1 resonance by October 2001. See Table 1 for explanation.

No.	Name	a_p [au]	e_p	I_p [°]	σ_a [au]	σ_e	σ_I [°]	t_{life} [$\times 10^6$ yr]	Other	D [km]
1362	Griqua	3.212	0.372	24.005	0.0018	0.0068	0.5716	149.5		29.9 ^a
3688	Navajo	3.213	0.507	4.688	0.0008	0.0009	0.5251	216.1	ν_{16}	6.3
4177	Kohman	3.231	0.320	15.997	0.0013	0.0011	0.1379	337.7	ν_{16}	17.4
11665	Dirichlet	3.219	0.225	17.953	0.0021	0.0069	0.5259	431.0		9.1
13963	1991 PT4	3.216	0.319	2.592	0.0014	0.0036	0.4092	352.2		11.0
24491	2000 YT123	3.222	0.204	1.430	0.0011	0.0022	0.2415	100.8		14.5
28459	2000 AW144	3.217	0.348	2.278	0.0019	0.0023	0.2412	190.0		11.0
29524	1998 AE	3.215	0.262	10.742	0.0020	0.0042	0.5550	509.1		12.0
	1999 NF10	3.211	0.278	0.696	0.0015	0.0044	0.2199	265.8	ν_{16}	8.3
	1999 XB143	3.183	0.431	9.403	0.0031	0.0645	1.3933	140.8	ν_5	17.4
	2000 HY9	3.214	0.294	0.905	0.0022	0.0034	0.1175	455.0	ν_{16}	6.9

^aIRAS diameter.

range (Fig. 2). This is rather due to the fact that the orbits shown in Fig. 5 are initial osculating elements, and thus cannot be directly compared to the pseudo-proper elements shown in Fig. 2.³

Because Fig. 5 does not allow a clear interpretation of the results, it is better to translate it into the space of pseudo-proper elements. To accomplish this, we used the following method.

(i) For each initial orbit, we determined the discrete time-series of the pseudo-proper elements a_p , e_p , I_p . The minimum of a and the

³Even when the initial orbits in Fig. 5 have $\sigma = 0$, $\varpi = \varpi_J$ and $\Omega = \Omega_J$, they are not coincident with the pseudo-proper elements computed at the same angular conditions. This is partially due to the fact that the initial orbital elements correspond to a specific epoch, while the pseudo-proper elements are computed over 10 Myr time-scales. Thus, for the orbits that chaotically evolve over such time-scales, the pseudo-proper elements do differ from the initial elements. Additional differences occur because the initial orbits shown in Fig. 5 are affected by the short-period terms related to the planetary orbital motions, and these short-period terms are filtered during the computation of the pseudo-proper elements.

maxima of e and I were computed every 0.1 Myr, using a running-time window of 10 Myr.

(ii) The space of pseudo-proper elements at $3.19 \leq a_p \leq 3.28$ au, $0.175 \leq e_p \leq 0.550$, and $0 \leq I_p \leq 10^\circ$, was divided in $18 \times 15 \times 1 = 270$ equal cells of size $\Delta a = 0.005$ au, $\Delta e = 0.025$, and $\Delta I = 10^\circ$.

(iii) For each orbit, we computed the time spent by the orbit’s pseudo-proper elements in each (a_i, e_j) cell during the simulation. This defined the time of residence, T_{ij} , of the orbit in the (a_i, e_j) cell. Note that orbits do not contribute to the time of residence if $I_p > 10^\circ$.

(iv) Finally, we computed the average of T_{ij} over all the orbits that visited the (a_i, e_j) cell during the simulation. If the (a_i, e_j) cell was never visited by any orbit, we set $T_{ij} = 0$.

The residence time defined in this way is a good indicator for the number of orbits that we expect to observe in each cell at a given time, and it proved to be quite robust when compared to alternate definitions.

As an example, the evolution of the pseudo-proper elements of four particles in our simulation is shown in Fig. 6. The cells are

Table 3. The stable asteroids (Zhongguos) observed in the 2 : 1 resonance by October 2001. See Table 1 for explanation. Asteroids labelled ν_{16} do not move in this secular resonance but are very close to it (i.e. $\Omega - \Omega_J$ circulates with a very long period).

No.	Name	a_p [au]	e_p	I_p [$^\circ$]	σ_a [au]	σ_e	σ_I [$^\circ$]	t_{life} [$\times 10^6$ yr]	Other	D [km]
3789	Zhongguo	3.236	0.222	2.642	0.0013	0.0015	0.2357	>520		20.0
11097	1994 UD1	3.233	0.267	2.564	0.0019	0.0013	0.1809	>520		12.6
11266	1981 ES41	3.222	0.272	2.770	0.0015	0.0018	0.2145	>520		11.0
11573	Helmholtz	3.221	0.293	3.688	0.0011	0.0019	0.1954	>520		15.8
14871	1990 TH7	3.217	0.280	2.137	0.0014	0.0028	0.2163	>520		11.0
16882	1998 BO13	3.228	0.271	2.138	0.0016	0.0022	0.2648	>520		11.0
18888	2000 AV246	3.231	0.263	1.689	0.0013	0.0013	0.1339	>520		11.5
22740	1998 SX146	3.237	0.230	3.735	0.0017	0.0009	0.2998	>520		13.8
24514	2001 BB58	3.229	0.278	1.392	0.0012	0.0018	0.1035	>520	ν_{16}	11.5
26112	1991 PG18	3.238	0.247	3.478	0.0014	0.0009	0.1738	>520		14.5
	1975 SX	3.223	0.217	2.808	0.0024	0.0051	0.2646	>520		8.3
	1998 DF14	3.223	0.306	1.490	0.0014	0.0024	0.1996	>520	ν_{16}	6.3
	1998 FP70	3.236	0.284	2.976	0.0011	0.0008	0.1039	>520	ν_{16}	10.0
	1998 KZ5	3.226	0.266	3.663	0.0014	0.0025	0.2988	>520		10.0
	1998 RO49	3.226	0.275	1.379	0.0025	0.0045	0.3900	>520	ν_{16}	7.2
	1999 RC168	3.225	0.221	1.312	0.0014	0.0024	0.1619	>520		9.1
	1999 XT23	3.234	0.274	2.098	0.0016	0.0009	0.0867	>520	ν_{16}	9.1
	1999 XZ55	3.222	0.221	1.802	0.0010	0.0020	0.6800	>520		10.5
	1999 XZ56	3.239	0.255	2.804	0.0016	0.0010	0.2460	>520		10.0
	2000 BC23	3.220	0.205	2.340	0.0025	0.0037	0.3565	>520		12.6
	2000 EF60	3.241	0.277	2.256	0.0017	0.0007	0.0282	>520	ν_{16}	5.0
	2000 FN44	3.219	0.242	3.093	0.0007	0.0027	0.3857	>520		12.0
	2000 SF206	3.235	0.263	4.261	0.0019	0.0013	0.1897	>520		6.0
	2000 UZ4	3.228	0.294	1.233	0.0022	0.0022	0.1427	>520	ν_{16}	8.3
	2000 UM53	3.231	0.275	5.093	0.0013	0.0011	0.2417	>520		8.7
	2001 AO22	3.232	0.281	2.586	0.0016	0.0007	0.1431	>520	ν_{16}	6.6

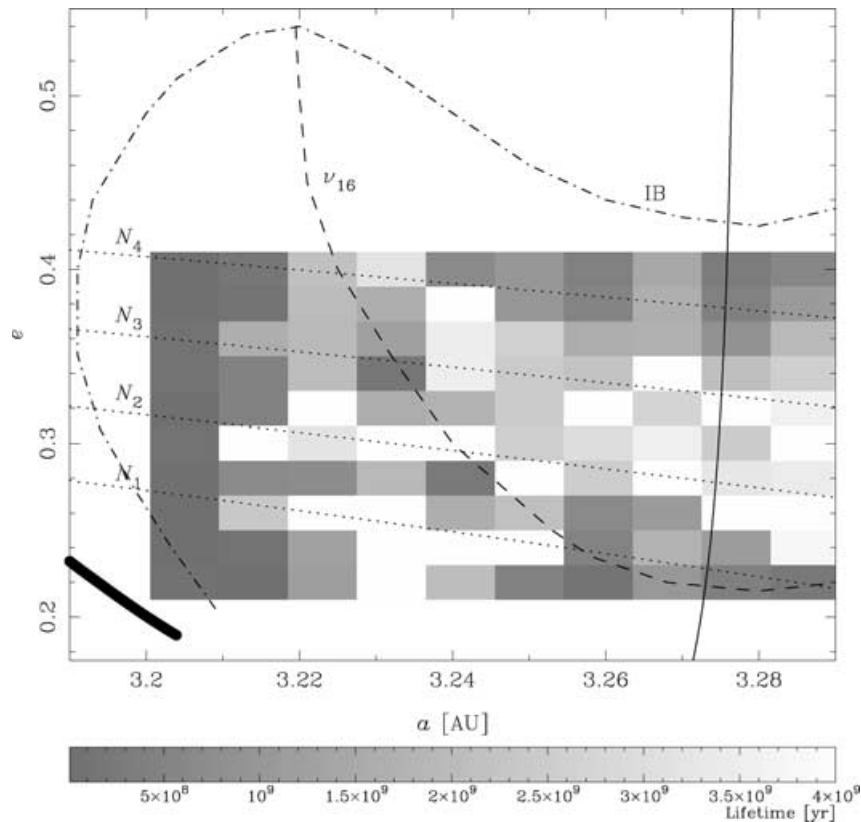


Figure 5. The lifetimes of the test orbits in our simulation. Each rectangle corresponds to one initial condition (with a , e in the centre of the rectangle). About 20 per cent of the test orbits survive over 4 Gyr.

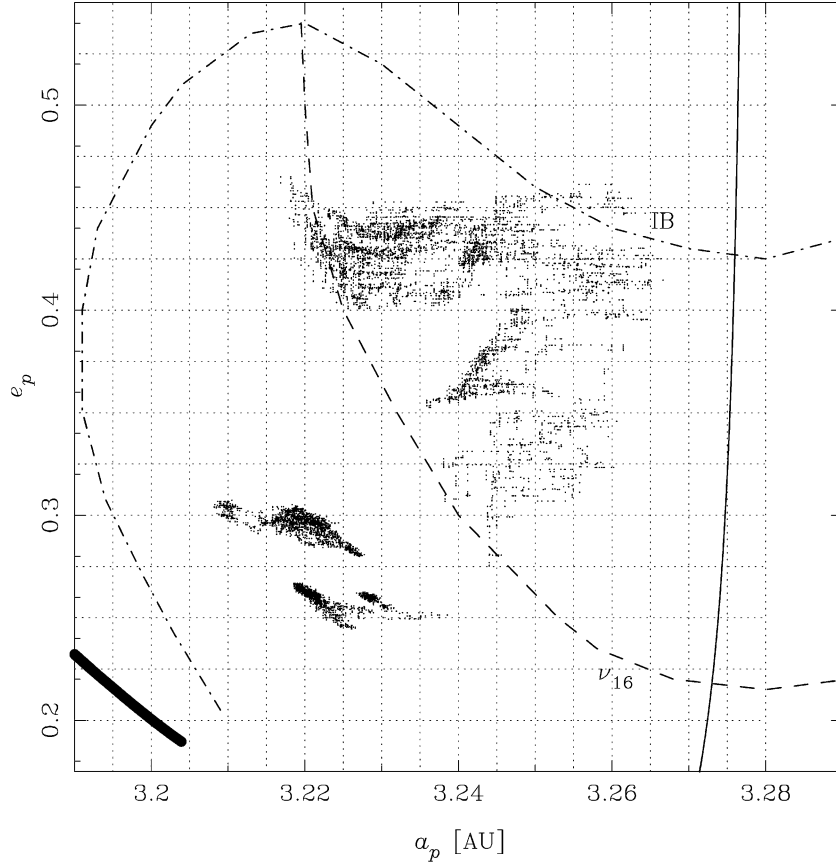


Figure 6. Evolution of resonant pseudo-proper elements of four test orbits in our simulation. Two orbits are located at the left side of the ν_{16} resonance, at about $e = 0.25$ and 0.3 , respectively. Other two orbits are (mostly) located at the right side of the ν_{16} resonance, above and below $e = 0.4$, respectively. The cells are indicated by dotted lines. The number of points in a cell is roughly proportional to the residence time in that cell.

indicated by dotted lines. The time of residence is approximately proportional to the number of points in each cell (compare to fig. 6 in Morbidelli 1996).

The times of residence in the 2:1 resonance are shown in Fig. 7. The colour scale is such that green/reddish cells have the shortest T_{ij} , blue/dark cells have the longest ones, and blank cells have zero residence times. T_{ij} is a qualitative indicator of the local chaotic diffusion in the i, j cell, for $I_p \leq 10^\circ$. This upper limit in the inclination was chosen so as to embrace in a single bi-dimensional portrait the typical values of I_p of the stable and marginally unstable resonant asteroids. In Fig. 7, the values of a_p and e_p of these asteroids are indicated by light-grey dots (Zhongguos) and dark-grey dots (Griquas), with their corresponding error bars.

Several features are seen in Fig. 7, as follows.

- (i) The residence time is short (~ 10 – 20 Myr) along a strip that follows the location of the ν_{16} secular resonance.
- (ii) The residence time is large at both sides of the ν_{16} resonance.
- (iii) The longest residence times (~ 1 Gyr) occur in the region between $3.22 < a_p < 3.24$ au and $0.22 < e_p < 0.30$. The stable asteroids (light-grey dots) are located in this region. We will call it Region Z, after Zhongguos. The mean residence time, averaged over all the cells in this region, is $\bar{T} = 500$ Myr.
- (iv) The cluster of stable asteroids around (11097) 1994 UD1 occupies the most stable place of Region Z, where they may survive over the age of the Solar system. However, asteroid (3789) Zhongguo is located on the brink of Region Z, and it could be unstable over billion-year time-scales (e.g. Morbidelli 1996).

- (v) The marginally unstable asteroids are located in the region $3.205 < a_p < 3.22$ au, where the mean residence time is $\bar{T} = 250$ Myr. We will call it Region G, after Griquas. Note, however, that (1362) Griqua and some other asteroids in that region have inclinations larger than 10° .

- (vi) The lower-right region in Fig. 7 shows many blank cells. The orbits started there have their inclinations and amplitudes of libration excited to large values on short time-scales ($\ll 10$ Myr). This behaviour occurred due to the ν_{16} resonance, located in this region.

- (vii) The upper and lower-left corners of Fig. 7, near the IB line, also show many blank cells. The orbits reaching these regions escaped from the resonance in time-scales much shorter than 10 Myr. We will call it Region C (as in ‘chaotic’).

- (viii) There is a large region at the right side of the ν_{16} resonance, between $3.225 < a_p < 3.26$ au, $e_p > 0.32$ and below the IB line, where the mean residence time is $\bar{T} = 130$ Myr. No asteroid is observed there. Following previous works (Nesvorný & Ferraz-Mello 1997a,b; Ferraz-Mello et al. 1998b), we will call it Region A.

- (ix) Some dark-grey dots seem to lie in more stable cells, while some light-grey dots seem to lie in less stable cells. These small discrepancies are due to the very different time-scales used to calculate the pseudo-proper elements (0.2 Myr) and the times of residence (4 Gyr).

It is worth noting that the maximum residence time of a single particle in a single cell was never longer than 2.6 Gyr. This means

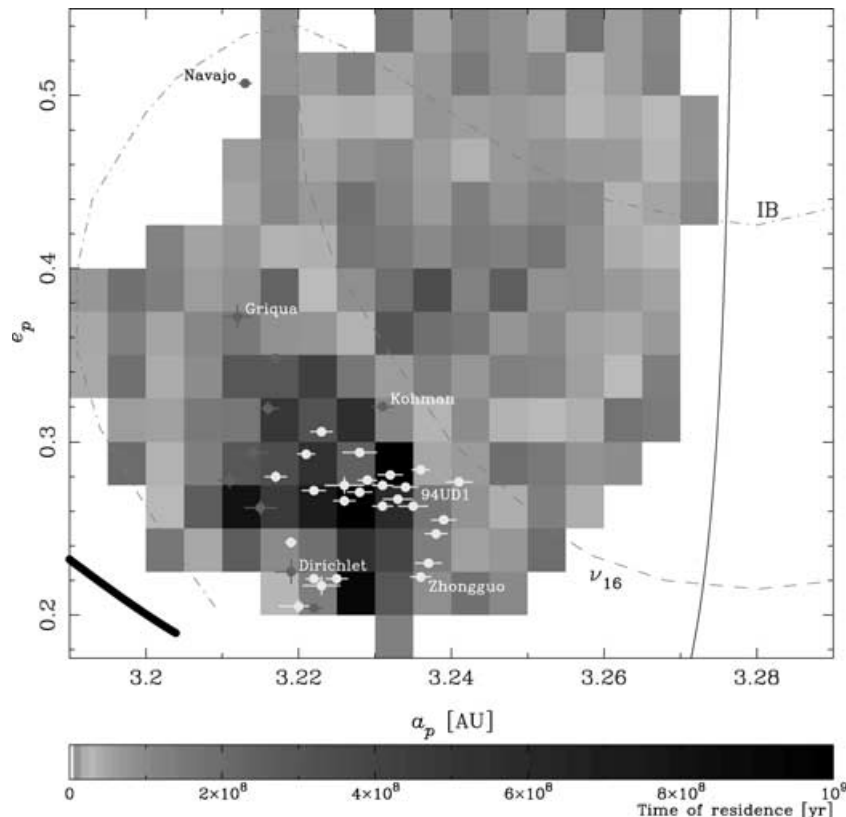


Figure 7. Residence times in the 2 : 1 mean motion resonance with Jupiter. The shortest residence times are $\ll 50$ Myr. Blank areas denote cells never visited by any orbit. Zhongguos and Griquas are denoted by light grey and dark grey dots, respectively. The agreement between the longest residence times and the locations of the real asteroids is remarkable. According to this, the cluster around (11097) 1994 UD1 could survive in the resonance over several Gyr. A colour version of this figure can be seen in the online version of the journal on *Synergy*.

that even the most stable orbits occupied more than one cell during the whole simulation. This result is highly relevant for the known theories of stable chaos. It provides evidence that some resonant orbits are stable over the age of the Solar system, even exhibiting an appreciable chaotic diffusion. Thus, the Zhongguos are likely to constitute a good example of stable chaos.

Our results indicate that the mean residence time in Region A is some 50 per cent of that in Region G, and about 25 per cent of that in Region Z. We have verified that these percentages are preserved when using alternate definitions of T_{ij} (e.g. the maximum in each cell, instead of the average). If only the orbits with $I_p < 5^\circ$ were contributing to the residence time, these percentages decrease to 40 and 15 per cent, respectively. This implies that a significant long-term excitation of the orbital inclinations occurs in Region A. But in any case, these percentages are not enough to justify the total lack of asteroids in Region A. Indeed, if the residence time is roughly proportional to the lifetime, we should observe a few asteroids in this region. In the following we will try to quantify this.

3.1 A random-walk model of the long-term dynamics

To describe the long-term chaotic diffusion in the resonance, we mounted a model of bi-dimensional random walk, using the residence times computed in the previous section. We used the idea that chaotic diffusion can be roughly modelled by a statistical process. Thus, a model of random walk, with adequate boundary conditions,

can be applied to huge sets of test orbits, and provides a detailed description of the chaotic diffusion at a very low computational cost (e.g. Nesvorný & Roig 2000, 2001).

Our model of random walk is very simple: an orbit entering the cell (a_i, e_j) , at time t , is randomly moved to one of its eight neighbouring cells at time $t + T_{ij}$, where T_{ij} is the residence time shown in Fig. 7. The model accounts for the following properties.

- (i) Orbits jump to a cell with smaller or higher e_p according to a probability $0 \leq p_e \leq 1$.
- (ii) Orbits jump to a cell with smaller or higher a_p with probability $p_a = 1$. This accounts for the fact that the resonant orbits roughly evolve along the lines of $N = \text{constant}$ (which correspond to $e_p \sim \text{constant}$).
- (iii) As a result of the symmetry of the resonant motion with respect to the resonance centre, orbits reaching a blank cell with $a_p > 3.25$ au are ‘reflected’, i.e. they are moved back to the last cell from which they have evolved
- (iv) Orbits reaching any other blank cell are deactivated from the simulation.

Using this Monte Carlo model, we simulated the evolution of a hypothetical primordial population of resonant asteroids over 4.5 Gyr. The initial orbits were set according to the distribution function described below.

We started assuming a uniform distribution of orbits in a, e, σ (with $I < 10^\circ$). This implies a non-uniform distribution in A_σ , because the orbits with large amplitudes of libration are more

frequent (Nesvorný, Roig & Ferraz-Mello 2000). Such distribution in A_σ can be computed in the averaged circular-planar restricted three-body problem: for different values of N (equation 4), we calculate the area enclosed by a resonant trajectory in the a, σ plane as

$$V(A_\sigma, N) = \int_0^{\tau_\sigma} [a(t) - a_{\text{res}}] \dot{\sigma} dt, \quad (5)$$

where $|a(0) - a_{\text{res}}| \propto A_\sigma$, and τ_σ is the libration period of the trajectory. Because A_σ is proportional to a_p and $N \sim e_p$, the area V is actually a function of the pseudo-proper elements: $V(a_p, e_p)$. Therefore, assuming a uniform density of orbits ρ inside the resonance, the number of orbits between a_p and $a_p + \Delta a$ at given e_p is:

$$\Delta n(a_p, e_p) = \rho \frac{dV(a_p, e_p)}{da_p} \Delta a \quad (6)$$

Δn grows with the amplitude of libration, as dV/da_p is an increasing function of A_σ . It also has a weak dependence with the eccentricity since, for fixed A_σ , V is smaller at larger N .

In our random-walk simulation, the uniform distribution of initial orbits in a, e, σ was represented by a uniform density $\rho = 1000$ orbits per cell. The corresponding distribution in pseudo-proper elements, determined from equation (6), is shown in Fig. 8(a). These initial orbits were evolved over 4.5 Gyr. We performed several simulations using different values of the probability p_e . This parameter can be adjusted to force the random walk to reproduce the shape of the actual resonant orbits (such as those shown in Fig. 6). Figs 8(b)–(d) show the final distribution of the orbits obtained from three simulations with $p_e = 0, 0.4$ and 1 , respectively. In panel (b), the orbits never jumped to smaller or higher e_p , while in panel (d), the orbits always jumped to smaller or higher e_p . The overall number of surviving orbits is smaller in this latter simulation, but the largest number of survivors always occurs in Region Z. Table 4 summarizes the results of these simulations. The first six rows give the average number of survivors per cell in Regions A and G, at different time-steps, normalized to the corresponding average number of survivors per cell in Region Z. The last row gives the actual averaged number of observed asteroids per cell.

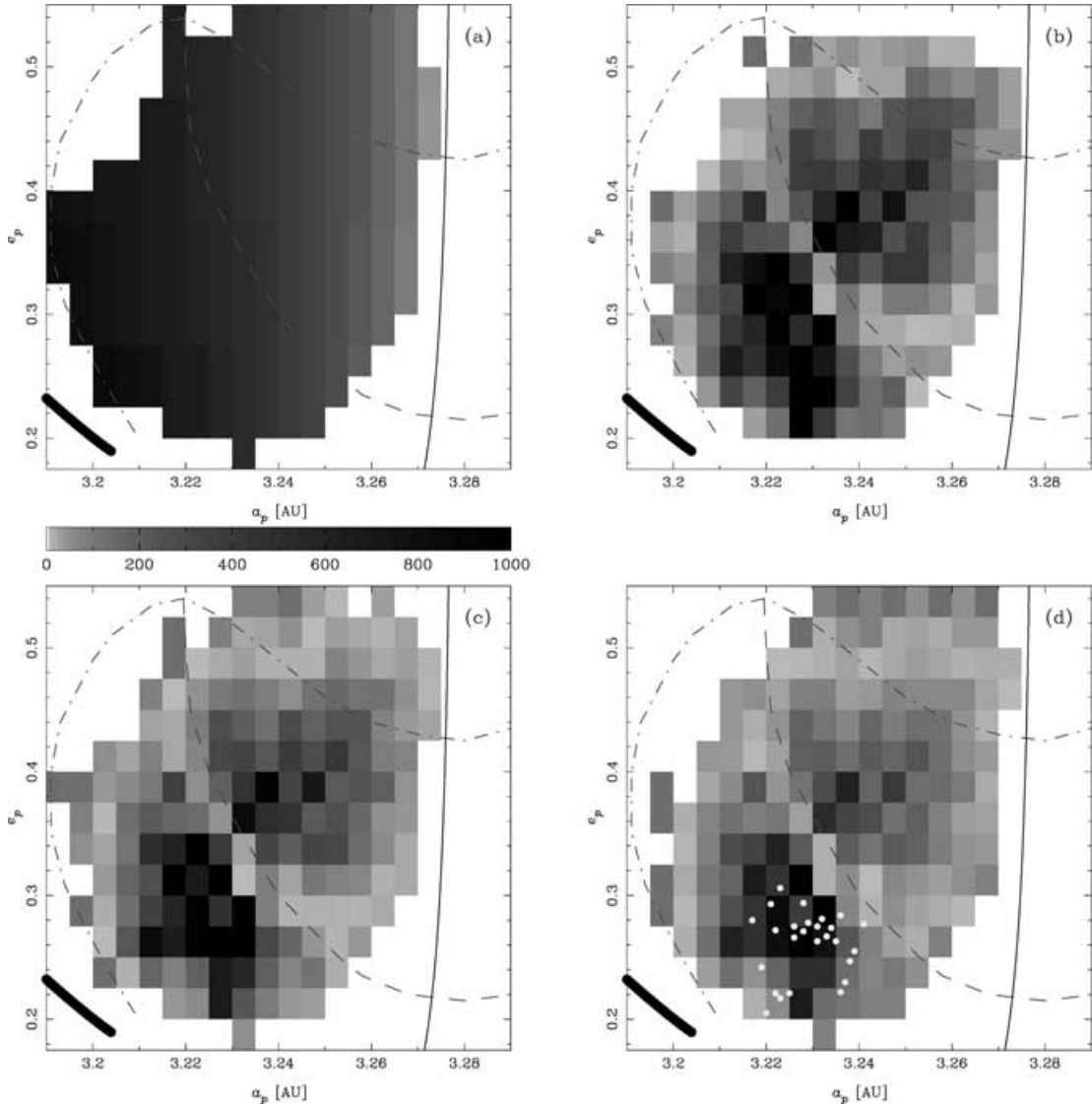


Figure 8. Initial distribution of the resonant orbits in our random-walk simulations (panel a), and final distributions at $t = 4.5$ Gyr using three different values of p_e : 0 (panel b), 0.4 (panel c), and 1 (panel d). The grey scale denotes the number of particles per cell. The darker regions are the most populated ones. Panel (d) shows the location of stable asteroids (dots). A colour version of this figure can be seen in the online version of the journal on *Synergy*.

Table 4. The number of surviving test orbits versus time in Regions A and G, for three different models of random walk (see text). The values are normalized to the number of surviving test orbits in Region Z. The last row shows the actual fractions of observed asteroids.

	Model $p_e = 0$		Model $p_e = 0.4$		Model $p_e = 1$	
	Region A	Region G	Region A	Region G	Region A	Region G
Initial	0.71	1.25	0.71	1.25	0.71	1.25
1.0 Gyr	0.49	0.68	0.58	0.71	0.57	0.70
2.0 Gyr	0.48	0.56	0.52	0.54	0.43	0.49
3.0 Gyr	0.47	0.48	0.47	0.49	0.37	0.42
4.0 Gyr	0.47	0.47	0.42	0.45	0.33	0.40
4.5 Gyr	0.47	0.46	0.40	0.45	0.32	0.38
Observed	0.00	0.38	0.00	0.38	0.00	0.38

Our random-walk model provides reasonable estimates for the observed ratio between the number of asteroids in Regions G and Z. This may indicate that the Griquas are the fugitives from the region of Zhongguos, which arrived to their present location as a result of the chaotic diffusion. This idea is supported by the fact that many Griquas have values of $I_p < 5^\circ$. However, the possible dynamical link between high-inclined Griquas and low-inclined Zhongguos is still an open problem.

On the other hand, the random-walk model fails to estimate the observed ratio between the number of asteroids in Regions A and Z. Our results indicate that there should be about eight asteroids in Region A which, up to now, were never observed. This is really puzzling. It has been proposed (Ferraz-Mello et al. 1998a; Roig & Ferraz-Mello 1999b) that this lack of asteroids is due to the presence in that region of three-body resonances involving the 5 : 2 mean motion near commensurability between Jupiter and Saturn (the so-called Great Inequality). Small changes in the orbits of the planets, as those arising from the planetary migration (Fernández & Ip 1984), can modify the period of the Great Inequality. This in turn, significantly enhance the chaotic diffusion of the orbits in Region A. However, it is not clear whether these slight changes of the Great Inequality also enhance the diffusion in Region Z (Nesvorný & Ferraz-Mello 1997b) or not (Roig & Ferraz-Mello 1999b). If the former is true, and Region Z can be also depleted by the changes in the Great Inequality, then the total lack of asteroids in Region A is unlikely to be explained by this mechanism.

Nevertheless, we cannot rule out the possibility of some dynamical mechanism acting in Region A that our models did not account for. As we have mentioned at the end of Section 3, the orbits in Region A have their inclinations largely excited. As our random-walk model is bi-dimensional and valid only for the small inclinations, it can be overestimating the number of surviving orbits in that region. In any case, the lack of asteroids in Region A is far from being explained, and more simulations (e.g. including planetary migration) are needed before we can draw any conclusions.

Our random-walk model also provides information about the origin of the strongly unstable asteroids in the 2 : 1 resonance. In Figs 8(b)–(d), a large number of orbits were deactivated when they reached a blank cell in the region near the instability border. Our simulations showed that, if n is the number of surviving test orbits in Region Z at $t = 4.5$ Gyr, then about $0.01 \times n$ orbits (from the total number of orbits initially in Region Z) became deactivated between 4.4 and 4.5 Gyr. These deactivated orbits contributed to the supply of the population of strongly unstable asteroids. Because we observe $n = 26$ Zhongguos at present, we conclude that about

0.3 objects, from the initial population in Region Z, should have escaped in the last 100 Myr, becoming strongly unstable. This is not enough to supply the 16 strongly unstable asteroids with lifetimes much smaller than 100 Myr that we observe at present. Thus, we conclude that strongly unstable asteroids are unlikely to have origin inside the 2 : 1 resonance. Their origin is most probably associated to extra-resonance sources (Roig et al., in preparation).

Both our N -body integrations and the random-walk simulations provide strong evidence that the Zhongguos, and particularly the cluster around (11097) 1994 UD1, can survive at their present location over the age of the Solar system. Our final conclusion is that, from the dynamical point of view, the Zhongguos could be the remnants of a large primordial resonant population.

3.2 The Yarkovsky effect and gravitational scattering

Up to now, we have analysed the long-term dynamics of the 2 : 1 resonance considering only gravitational perturbations from the major planets. We will discuss here the role of other perturbations, such as the Yarkovsky effect and the scattering by main belt asteroids, which introduce changes on the basic resonant dynamics.

The Yarkovsky effect arises from the thermal recoil suffered by a rotating body, which translates into an increase or decrease of its orbital energy (Afonso, Gomes & Florczak 1995; Farinella & Vokrouhlický 1999). There are two variants of the effect: the diurnal effect, resulting from the rotation of the body, and the seasonal effect, resulting from its orbital motion around the Sun (Rubincam 1995). While the former effect can increase or decrease the orbital energy depending on the sense of rotation, the latter one always decreases the energy. For non-resonant asteroids, the combination of both effects translates into a net drift in a , while e and I remain nearly unchanged. Such drift plays an important role in spreading the members of asteroidal families in the main belt (Bottke et al. 2001; Nesvorný et al. 2002). Among other parameters, the Yarkovsky effect mainly depends on the diameter of the body: the larger the body, the smaller the effect. Actually, the effect is relevant only for objects with $D < 20$ km.

We have modified the symplectic integrator SWIFT to include the components of the Yarkovsky acceleration according to the formulas of Vokrouhlický, Milani & Chesley (2000). Using this modified code, we integrated 50 test orbits with initial conditions in the range $3.205 \leq a \leq 3.286$ au, and $0.22 \leq e \leq 0.40$. These initial conditions were the same used in our previous simulation without the Yarkovsky effect (Section 3). The simulation spanned 1 Gyr. The physical parameters of the bodies were chosen similar to those corresponding to regolith-covered asteroids (e.g. Farinella, Vokrouhlický & Hartmann 1998). The test bodies had a diameter $D = 5$ km, in agreement with the lower limit of the observed sizes of Zhongguos (Section 4), and rotational period of 20 h (Angeli, private communication). The spin components (s_x , s_y , s_z) of each body were chosen at random, with $s_z > 0$ (i.e. prograde rotation), and were kept fixed during the simulation. With this choice of parameters, the diurnal effect dominated over the seasonal, causing a net energy gain.⁴

52 per cent of the test orbits survived the simulation after 1 Gyr of evolution. This number should be compared with 58 per cent of surviving orbits when the Yarkovsky effect was not included. We computed the time-series of pseudo-proper elements in both simulations, and calculated their linear best-fits and their standard

⁴The term ‘energy’ must be understood as the orbital energy of the resonant orbit, which differs from the classical $-1/2a$ energy of a non-resonant orbit.

deviations. These quantities provide information about the chaotic diffusion, and we refer to them as *diffusion parameters* (e.g. Nesvorný et al. 2002). In the simulation including the Yarkovsky effect, we observe a trend to slightly larger values of these diffusion parameters, especially for e_p .⁵ However, the overall effect is actually very small. We conclude that the Yarkovsky effect does not seem to significantly change the long-term dynamics inside the 2 : 1 resonance, at least for asteroids larger than 5 km.

Another effect that could introduce changes in the long-term dynamics is the gravitational scattering, i.e. the perturbations caused by close encounters with other asteroids (excluding the possibility of impact and fragmentation). Both Zhongguos and Griquas potentially suffer close encounters with main belt asteroids. Recent studies (Nesvorný et al. 2002; Carruba et al., in preparation) indicate that only the largest asteroids (Ceres, Pallas and Vesta) seem to have a dominant scattering effect. Actually, the Zhongguos can reach values of q as small as 2.35–2.50 au, which means that they cross the orbits of Ceres and Pallas. According to Monte Carlo simulations (Bottke, private communication), close encounters between an asteroid in 2 : 1 resonance and Ceres are responsible for a change in a_p of less than $1/100$ au Gyr⁻¹. We then conclude that gravitational scattering is inefficient to significantly destabilize the Zhongguos.

4 SIZE DISTRIBUTION

The size distribution of an asteroidal population tells us about its collisional evolution. We know, for example, that a population formed by the breakup of a single asteroid tends to have a quite steep size distribution (Petit & Farinella 1993; Michel et al. 2001). We also know that the subsequent collisional evolution of this population will make its size distribution more shallow (Dohnanyi 1969). We discuss here the observed size distribution of the Zhongguos and its implications for the origin of these asteroids.

Following Muinonen, Bowell & Lumme (1995), we estimated the sizes of the 2 : 1 resonant asteroids from their albedo. Asteroid (1362) Griqua has a known *IRAS* albedo $A = 0.0667$. For the asteroids with unknown albedo we assumed $A = 0.05$. This value was a good compromise between the typical albedos of C-type and D-type asteroids, which are the most frequent types in the outer asteroid belt ($a > 2.8$ au). The estimated diameters are listed in Tables 1, 2 and 3. All the asteroids but (1362) Griqua are smaller than 22 km. According to Farinella & Davis (1992), the collisional lifetimes of such bodies is ~ 1 Gyr. Then, most of them are unlikely to be primordial resonant asteroids.

The cumulative size distributions of the resonant asteroids are shown in Fig. 9. The full line is the size distribution of the Zhongguos. The dashed line is the distribution of all the 2 : 1 resonant asteroids (Zhongguos + Griquas + strongly unstable). The dotted-dashed line is the size distribution of Themis family, which is shown here for purposes of comparison. The dotted lines are the power-law $N(>D) \propto D^\alpha$ best-fittings (e.g. Petit & Farinella 1993).

The most remarkable feature in Fig. 9 is an extreme steepness of the size distribution of the Zhongguos. Collisional models show

⁵This behaviour may be described by simple analytical models (e.g. Gomes 1995, 1997a) using the theory of adiabatic invariants. In short, non-conservative forces outside the resonance cause an increase/decrease of the averaged semi-major axis. However, inside the resonance, the averaged semi-major axis is locked, and the gain/loss of energy is transferred to the other momenta, that is e and I .

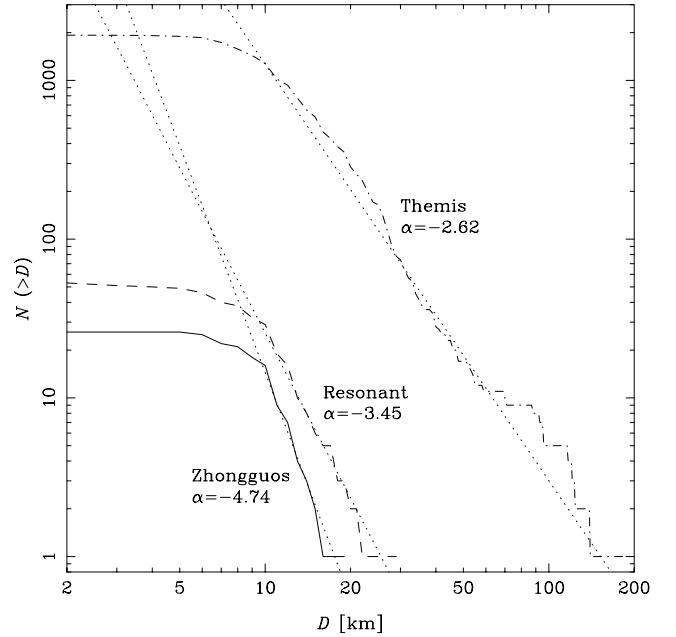


Figure 9. The size distributions of the resonant asteroids in the Hecuba gap (solid line and dashed line), and the size distribution of Themis family (dot-dashed line). For Zhongguos and Resonant asteroids, the power-law $N(>D) \propto D^\alpha$ best-fits (dotted lines) were computed for $D \geq 10$ km. For the Themis family, the power-law was fitted in the range $24 \leq D \leq 70$ km. The corresponding values of α are indicated. The diameters were computed either from the *IRAS* albedo when available, or assuming $A = 0.05$ when the *IRAS* albedo was unknown.

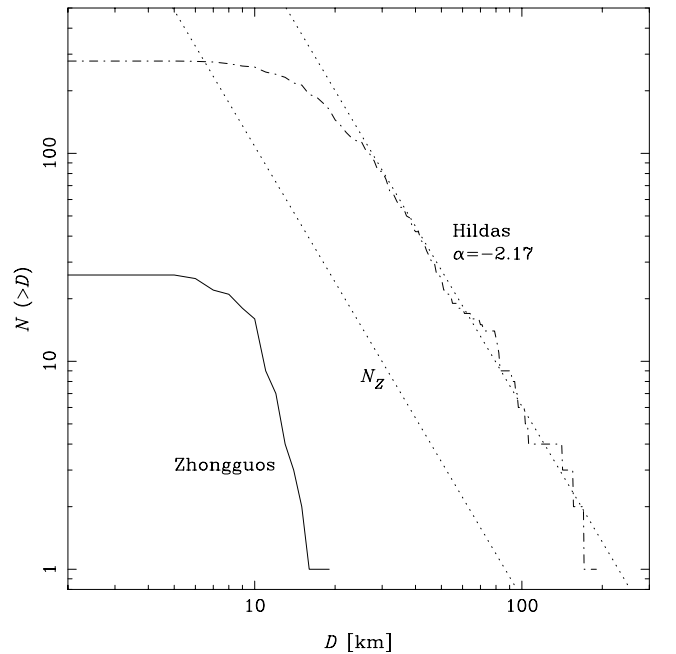


Figure 10. The size distributions of the Zhongguos (solid line) and the Hildas (dashed line). In the latter case, the power-law $N(>D) \propto N^\alpha$ was fitted in the range $40 \leq D \leq 126$ km. The dotted line labelled N_Z is the power-law scaled down to the 2 : 1 resonance (equation 7). The diameters were computed either from the *IRAS* albedo, or assuming $A = 0.05$ when the *IRAS* albedo was unknown.

that a collisionally relaxed population tends to have a power-law distribution with $\alpha \sim -2.5$ (Dohnanyi 1969). Then, $\alpha = -4.74$ may indicate that the Zhongguos are a ‘fresh’ population (Michel et al. 2001), which formed very recently and did not have enough time to evolve to a more shallow distribution. When the whole resonant population is considered, the size distribution becomes more shallow as a result of the contribution of two large asteroids: (1362) Griqua and (1922) Zulu. However, the steepness of the size distribution is still remarkable, especially if compared to the size distribution of Themis family.

Could these values of α be a consequence of the observational bias? The diameters of Zhongguos and Griquas are below the limit of observational completeness for that region of the asteroid belt (≈ 24 km, Jedicke & Metcalfe 1998). Thus, the known resonant population is largely incomplete. It is, however, difficult to attribute the steep size distribution of the resonant asteroids to the observational bias: such bias would preferably affect the small-sizes tail of the distribution, rather than the large-sizes end. In fact, we may expect that the discovery of new objects will tend to make the size distribution even steeper. Note, for example, that about 60 per cent of the Zhongguos have been discovered in the last 5 yr, all of them having diameters smaller than 14 km (see last column of Table 3). Then, it seems unlikely that $\alpha = -4.74$ be a result of the observational bias.

4.1 Zhongguos: a scaled-down analogue of the Hildas?

In Section 3, we concluded that, due to their long lifetimes, the Zhongguos can be the remnants of a primordial population of resonant bodies. It is then natural to compare them with the Hilda group in the 3 : 2 resonance with Jupiter.

The Hilda group accounts for about 260 asteroids which occupy the most stable region inside the 3 : 2 resonance. They can survive in the resonance over time-scales of billions of years (Nesvorný & Ferraz-Mello 1997b; Ferraz-Mello et al. 1998b). The Hildas constitute a primordial resonant population: the group includes several large asteroids ($D > 100$ km), whose collisional lifetimes are longer than the age of the Solar system. Moreover, the 3 : 2 resonance is surrounded by largely depleted chaotic regions (Wisdom 1980; Murray & Holman 1997); thus, the Hildas most probably formed inside the resonance. This idea is reinforced by the fact that most Hildas belong to the same taxonomic class, D-type, so they have the same chemical composition.

How would the Hildas look like if they were in the 2 : 1 resonance? Would they reproduce the present size distribution of the Zhongguos? To answer these questions we have to account for the different volumes occupied by the Hildas and the Zhongguos in their respective resonances. The Hildas occupy a large region in the core of the 3 : 2 resonance, while the Zhongguos concentrate in a small region of the 2 : 1 resonance. If $N_H(>D)$ is the cumulative size distribution of the Hildas, we can scale it down to the size distribution of the Zhongguos, $N_Z(>D)$, using:

$$N_Z(>D) = \frac{\Delta V_Z}{\Delta V_H} N_H(>D) \quad (7)$$

where

$$\Delta V = \frac{dV}{da_p} \Delta a_p \Delta e_p \Delta I_p \quad (8)$$

is the volume occupied in the space of pseudo-proper elements by each population. Table 5 gives the assumed values of Δa_p , Δe_p and ΔI_p . These values were determined empirically from the orbital

Table 5. The values of the quantities used in equations (7) and (8). The values of dV/da_p were computed from equation (5) (see text).

	Δa_p [au]	Δe_p	ΔI_p [°]	dV/da_p [rad]
Zhongguos	0.02	0.05	5	2.8
Hildas	0.05	0.2	10	1.2

distribution of the Zhongguos and Hildas. The derivatives dV/da_p were computed using equation (5), assuming $I_p = 0$ and a_p, e_p equal to the mean values ($\langle a_p \rangle, \langle e_p \rangle$) of each population.

Fig. 10 shows the size distribution of the Hildas (dashed line) and its power-law best-fitting (dotted line). This power-law has been scaled down to the 2 : 1 resonance using equation (7) (dotted line labelled N_Z). The present size distribution of the Zhongguos (full line) is shown for comparison. We can see that there are fewer Zhongguos than would be expected from the scaled-down distribution of the Hildas. The Zhongguos seem to be more depleted than we would expect from their stability over the age of the Solar system. They have also a much steeper size distribution. According to the scaled-down distribution, there should be a couple of Zhongguos larger than 50–60 km which are not actually observed.

What are the possible reasons for the contrasting populations of Zhongguos and Hildas?

The Zhongguos are about 20 times more depleted than the scaled-down size distribution of the Hildas, and it is highly improbable that chaotic diffusion and/or collisional comminution may account for such difference. Moreover, these processes cannot explain the steep size distribution of the Zhongguos either. Indeed, chaotic diffusion has no preference for sizes, and cannot justify the lack of large Zhongguos relative to the small ones. Collisional disruption may have eliminated the large Zhongguos and created smaller ones. Actually, the collisional evolution in the 2 : 1 has been much more active than in the 3 : 2 resonance.⁶ However, the trend in this case would be towards a more shallow size distribution of the Zhongguos with respect to that of the Hildas, while in Fig. 10 we observe the opposite trend.

The difference in the size distributions cannot be attributed to the observational bias either. Actually, we are not scaling down the size distribution of the Hildas, but rather its power-law best fitting. This power law has been fitted within the range of observational completeness of the Hilda group ($D > 50 \pm 10$ km; Mothé-Diniz, personal communication). Therefore, the scaled-down size distribution is not affected by the observational bias.

On the other hand, the distinct size distributions of Zhongguos and Hildas may be related to the early history of these populations. The formation processes and the formation efficiency in both resonances may have been very different, and the number of bodies in the primordial resonant populations may have substantially differed. Moreover, dynamical mechanisms like the planetary migration (Gomes 1997b; Liou & Malhotra 1997), or the excitation by a swarm of planetesimals (Petit, Morbidelli & Valsecchi 1999; Petit, Morbidelli & Chambers 2001), probably affected the main asteroid belt in a different way than they affected the outer belt. These

⁶While the Zhongguos may collisionally interact with main belt asteroids (Section 3.2), the 3 : 2 resonance is more isolated from the main belt, and the collisional history of the Hildas has been mainly dictated by their mutual collisions (Dell’Oro et al. 2001).

mechanisms may have contributed to the early clearing of the 2 : 1 resonance, while leaving the 3 : 2 resonance almost untouched. Thus, the original size distribution of the asteroids in the 2 : 1 resonance may have been very different from that of the Hildas. Nevertheless, this does not seem to explain the presently steep size distribution of the Zhongguos. We are then induced to conclude that, *in spite of their long-term stability, the Zhongguos may not be the remnants of a primordial resonant population.*

5 CONCLUSIONS

The asteroidal population in the 2 : 1 resonance with Jupiter (Hecuba gap) accounts for 53 observed asteroids by 2001 October. These bodies can be divided in three sub-populations:

- (i) the Zhongguos or stable asteroids, which lifetimes in the resonance are larger than ~ 500 Myr,
- (ii) the Griquas or marginally unstable asteroids, with lifetimes between 100 and 500 Myr, and
- (iii) the strongly unstable asteroids, which escape from the resonance in less than 100 Myr.

The Zhongguos account for about half of the observed population. They are located in the most stable place of the resonance, at low inclinations ($< 5^\circ$). Many of them form a tight cluster in the space of proper elements, around asteroid (11097) 1994 UD1. Most Zhongguos can survive in the resonance over the age of the Solar system. The long-term stability of these asteroids is neither affected by the Yarkovsky effect, nor by the gravitational scattering by main belt asteroids. The Zhongguos may actually be the remnants of a primordial resonant population of asteroids, like the Hildas in the 3 : 2 resonance.

However, unlike the Hildas, the Zhongguos have a very steep size distribution. This is incompatible with a collisionally relaxed population, and suggests that the Zhongguos might be the outcomes of a collisional event. In this context, the steepness would be a natural consequence of the breakup of the parent body, and a size distribution $\propto D^{-4.74}$ may indicate a recent breakup (Michel et al. 2001). The steepness may also indicate a cratering event, not necessarily recent. For example, the Vesta family, which has a size distribution $\propto D^{-5.3}$, was formed by a cratering impact on asteroid (4) Vesta about 1 Gyr ago (Asphaug 1997; Thomas et al. 1997).

An hypothetical cratering/breakup may have occurred inside the 2 : 1 resonance. In this case, the parent body would be either a primordial resonant asteroid or a body temporarily captured in the resonance. The cratering/breakup would likely result from the collision of this resonant parent body with a main belt asteroid. According to the lifetimes in Regions A and G, this cratering/breakup should have happened at least 1–2 Gyr ago, to allow the depletion of the fragments other than those in the Zhongguos region.

The cratering/breakup may also have happened in the neighbourhood of the 2 : 1 resonance. Actually, it has been proposed that the Zhongguos are fragments of the breakup that formed the Themis family (Morbidelli et al. 1995; Moons et al. 1998). In this case, several small fragments would have been injected in the resonance about 2 Gyr ago (Marzari et al. 1995). However, it is not clear whether or not such a breakup event can generate the large ejection velocities ($\gg 200 \text{ m s}^{-1}$) necessary to reach the Zhongguos region inside the 2 : 1 resonance. On the other hand, a cratering impact on a large asteroid near the border of the resonance can generate many small fragments, with the required large ejection velocities (Asphaug 1997). A detailed treatment of this problem is left to a forthcoming paper (Roig et al., in preparation).

The Griquas are located in a region of transition between the stable and the strongly unstable regions of the resonance. Their actual origin is not clear. They may have formed together with the Zhongguos by the breakup of a large asteroid inside the resonance. In this case, asteroid (1362) Griqua could be the parent body. Actually, the Griquas seem to be the fugitives from the Zhongguos' region, which arrived at their present location as a result of the chaotic processes inside the 2 : 1 resonance.

The strongly unstable asteroids are located near the borders of the resonance. As a result of their very short lifetimes, they must be continuously re-supplied to keep a steady number of such bodies in the resonance. The strongly unstable asteroids can be generated only from outside the 2 : 1 resonance. The chaotic diffusion in the neighbourhood of the 2 : 1 resonance, the Yarkovsky effect and other dynamical mechanisms may be responsible for the origin of these asteroids (Roig et al., in preparation).

There is a large region at the middle of the 2 : 1 resonance (Region A) which is totally depleted of asteroids. This is puzzling because there is no evident dynamical reason for the lack of asteroids in that region. If the Zhongguos were primordial resonant asteroids, then some dynamical mechanism must help to deplete Region A over the age of the Solar system without causing a similar depletion of the Zhongguos. However, if the Zhongguos were formed by a collisional event, the lack of asteroids in Region A can also be explained if the outcomes of such event never reached that region. The problem is open for future studies.

While the dynamics of the Zhongguos favour the idea of a primordial resonant population, their size distribution points rather to a recent origin. We actually believe that a cratering impact on a near-resonant asteroid, or even on a body temporarily captured in the 2 : 1 resonance, may have been injected the Zhongguos in their present location several hundreds of million years ago. The spectroscopic observations to determine the taxonomy of these asteroids can provide valuable evidence about their origin, and are especially urged.

Nevertheless, the above hypothesis opens a big question: if the remnants of a primordial resonant population may survive up to the present, and the Zhongguos are not such remnants, where are they? The answer to this question may lastly be in cosmogonic or early processes (e.g. planetary migration, planetesimal excitation) that are worthy of future analysis.

ACKNOWLEDGMENTS

This work has been supported by the São Paulo State Science Foundation (FAPESP). Numerical simulations were performed using the resources of the LCCA/USP. FR thanks the Southwest Research Institute at Boulder, Colorado, for hosting his visit during the final stages of this work. Fruitful discussions with W. Bottke, D. Durda, P. R. Holvorcem and A. Morbidelli helped to improve the contents of this paper, and are highly appreciated.

REFERENCES

- Afonso G., Gomes R., Florczak M., 1995, *Planetary Space Sci.*, 43, 787
- Asphaug E., 1997, *Meteor. Planet. Sci.*, 32, 965
- Benz W., Asphaug E., 1999, *Icarus*, 142, 5
- Bien R., Schubart J., 1987, *A&A*, 175, 292
- Bottke W. F., Vokrouhlický D., Brož M., Nesvorný D., Morbidelli A., 2001, *Sci*, 294, 1693
- Dell'Oro A., Marzari F., Paolicchi P., Vanzani V., 2001, *A&A*, 366, 1053
- Dohnanyi J., 1969, *J. Geophys. Res.*, 74, 2531

- Farinella P., Davis D., 1992, *Icarus*, 97, 111
 Farinella P., Vokrouhlický D., 1999, *Sci*, 283, 1507
 Farinella P., Vokrouhlický D., Hartmann W. K., 1998, *Icarus*, 132, 378
 Fernández J., Ip W.-H., 1984, *Icarus*, 58, 109
 Ferraz-Mello S., 1994, *AJ*, 108, 2330
 Ferraz-Mello S., Michtchenko T. A., Roig F., 1998a, *AJ*, 116, 1491
 Ferraz-Mello S., Michtchenko T. A., Nesvorný D., Roig F., Simula A., 1998b, *Planetary Space Sci.*, 46, 1425
 Gomes R., 1995, *Icarus*, 115, 47
 Gomes R., 1997a, *AJ*, 114, 2166
 Gomes R., 1997b, *AJ*, 114, 396
 Jedicke R., Metcalfe T. S., 1998, *Icarus*, 131, 245
 Kirkwood D., 1867, *Meteoric Astronomy*. J. B. Lippincott, Philadelphia
 Knežević Z., Milani A., 2000, *Cel. Mech. Dyn. Astron.*, 78, 17
 Levison H. F., Duncan M. J., 1994, *Icarus*, 108, 18
 Liou J. C., Malhotra R., 1997, *Sci*, 275, 375
 Malhotra R., 1995, *AJ*, 110, 420
 Malhotra R., 1996, *AJ*, 111, 504
 Marzari F., Scholl H., 1998a, *Icarus*, 131, 41
 Marzari F., Scholl H., 1998b, *A&A*, 339, 278
 Marzari F., Davis D., Vanzani V., 1995, *Icarus*, 113, 168
 Michel P., Benz W., Tanga P., Richardson D. C., 2001, *Sci*, 294, 1696
 Michtchenko T. A., Ferraz-Mello S., 1995, *A&A*, 303, 945
 Michtchenko T. A., Ferraz-Mello S., 1996, *A&A*, 310, 1021
 Michtchenko T. A., Ferraz-Mello S., 1997, *Planetary Space Sci.*, 45, 1587
 Milani A., Knežević Z., 1990, *Cel. Mech. Dyn. Astron.*, 49, 347
 Milani A., Knežević Z., 1994, *Icarus*, 107, 219
 Moons M., Morbidelli A., Migliorini F., 1998, *Icarus*, 135, 458
 Morbidelli A., 1996, *AJ*, 111, 2453
 Morbidelli A., 1997, *Icarus*, 127, 1
 Morbidelli A., Moons M., 1993, *Icarus*, 103, 99
 Morbidelli A., Nesvorný D., 1999, *Icarus*, 139, 295
 Morbidelli A., Zappalà V., Moons M., Cellino A., Gonczi R., 1995, *Icarus*, 118, 132
 Muinonen K., Bowell E., Lumme K., 1995, *A&A*, 293, 948
 Murray N. W., Holman M. J., 1997, *AJ*, 114, 1246
 Nesvorný D., Ferraz-Mello S., 1997a, *A&A*, 320, 672
 Nesvorný D., Ferraz-Mello S., 1997b, *Icarus*, 130, 247
 Nesvorný D., Roig F., 2000, *Icarus*, 148, 282
 Nesvorný D., Roig F., 2001, *Icarus*, 150, 104
 Nesvorný D., Roig F., Ferraz-Mello S., 2000, *AJ*, 119, 953
 Nesvorný D., Morbidelli A., Vokrouhlický D., Bottke W. F., Brož M., 2002, *Icarus*, 157, 155
 Petit J. M., Farinella P., 1993, *CMDA*, 57, 1
 Petit J. M., Morbidelli A., Valsecchi G., 1999, *Icarus*, 141, 367
 Petit J. M., Morbidelli A., Chambers J., 2001, *Icarus*, 153, 338
 Roig F., Ferraz-Mello S., 1999a, in Henrard J., Ferraz-Mello S., eds, *Proc. IAU Coll. 172, Impact of Modern Dynamics in Astronomy*. Kluwer, Dordrecht, p. 387
 Roig F., Ferraz-Mello S., 1999b, *Planetary Space Sci.*, 47, 653
 Rubincam D. P., 1995, *J. Geophys. Res.*, 100, 1585
 Schubart J., 1982, *A&A*, 114, 200
 Thomas P., Binzel R., Gaffey R., Storrs A., Wells E., Zellner B., 1997, *Sci*, 277, 1492
 Vokrouhlický D., Milani A., Chesley S., 2000, *Icarus*, 148, 118
 Wisdom J., 1980, *AJ*, 85, 1122
 Zappalà V., Cellino A., Farinella P., Knežević Z., 1990, *AJ*, 100, 2030
 Zappalà V., Bendjoya Ph., Cellino A., Farinella P., Froeschlé C., 1995, *Icarus*, 116, 291

This paper has been typeset from a $\text{\TeX}/\text{\LaTeX}$ file prepared by the author.